

Anionic Poly(*p*-Phenylenevinylene)/Layered Double Hydroxide Ordered Ultrathin Films with Multiple Quantum Well Structure: A Combined Experimental and Theoretical Study

Dongpeng Yan,[†] Jun Lu,^{*,†} Jing Ma,[‡] Min Wei,^{*,†} Xinrui Wang,[†] David G. Evans,[†] and Xue Duan[†]

[†]State Key Laboratory of Chemical Resource Engineering, Beijing University of Chemical Technology, Beijing, 100029, P. R. China and [‡]School of Chemistry and Chemical Engineering, Institute of Theoretical and Computational Chemistry, Key Laboratory of Mesoscopic Chemistry of MOE, Nanjing University, Nanjing, 210093, P.R. China

Received November 8, 2009. Revised Manuscript Received January 8, 2010

The sulfonated phenylenevinylene polyanion derivate (APPV) and exfoliated Mg–Al-layered double hydroxide (LDH) monolayers were alternatively assembled into ordered ultrathin films (UTFs) employing a layer-by-layer method, which shows uniform yellow luminescence. UV–vis absorption and fluorescence spectroscopy present a stepwise and regular growth of the UTFs upon increasing deposited cycles. X-ray diffraction, atomic force microscopy, and scanning electron microscopy demonstrate that the UTFs are orderly periodical layered structure with a thickness of 3.3–3.5 nm per bilayer. The APPV/LDH UTFs exhibit well-defined polarized photoemission characteristic with the maximum luminescence anisotropy of ~0.3. Moreover, the UTF exhibit longer fluorescence lifetime (3–3.85-fold) and higher photostability than the drop-casting APPV film under UV irradiation, suggesting that the existence of a LDH monolayer enhances the optical performance of the APPV polyanion. A combination study of electrochemistry and periodic density functional theory was used to investigate the electronic structure of the APPV/LDH system, illustrating that the APPV/LDH UTF is a kind of organic–inorganic hybrid multiple quantum well (MQW) structure with a low band energy of 1.7–1.8 eV, where the valence electrons of APPV can be confined into the energy wells formed by the LDH monolayers effectively. Therefore, this work not only gives a feasible method for fabricating a luminescence ultrathin film but also provides a detailed understanding of the geometric and electronic structures of photoactive polyanions confined between the LDH monolayers.

Introduction

The last 2 decades have witnessed considerable research advances of the luminescent π -conjugated polymers (π -CP) since the first discovery of light-emitting phenomena of poly(*p*-phenylenevinylene) (PPV) by R. H. Friend et al. in 1990.¹ Tremendous attention has been focused on the promising applications of π -CP in the field of optoelectronic devices, such as light-emitting diodes² and photovoltaic cells.³ To date, however, the luminescence performances based on the π -CP film are still greatly limited by their relatively short service lifetime and unsatisfactory stability. Moreover, compared with their solution counterparts,⁴ the poor luminescent properties, for example, the phenomena of fluorescence red-shift, broadening, or even quenching, can still be found in many of the solid state π -CP films owing to a very high tendency of the formation of molecular aggregates based on the aromatic π – π interactions. It is of prime importance for the application of luminescent π -CP films to obtain excellent optical properties and to enhance its thermal or optical stability. Accordingly, great efforts have been devoted to

design and synthesize new types of π -CP derivatives to meet these demands;⁵ unfortunately, the time-consuming synthesis process and relative low yield often restrict their application. Recently, electrostatic layer-by-layer (LBL) deposition technique has been widely employed into the preparation of polyanion/polycation thin films to tune and control optical properties of π -CP due to its operational simplicity, whereas considerable interlayer penetration between adjacent polymer layers might occur for the π -CP multilayer films assembled by the LBL technique,⁶ which is detrimental for the improvement of their optical properties. Therefore, it is highly desirable to find suitable building blocks for π -CP films to overcome these limitations and to fabricate a novel orderly assembled luminescent system, which can effectively isolate the π -CP chromophores and reduce their π – π stacking interaction.

Layered double hydroxides (LDHs) are a large class of typical inorganic layered host materials, the general formula of which can be described as $[M^{II}_{1-x}M^{III}_x(OH)_2]^{z+}A^{n-}_{z/n} \cdot yH_2O$. M^{II} and M^{III} are divalent and trivalent metals ions, respectively; A^{n-} are the guest anions presenting between the hydroxide layers.⁷ Recently, alternative assembly of LDH monolayers and organic polyanions with LBL technique came into reality in the pioneering work of Sasaki et al.,⁸ which facilitated a new type of functional hybrid

*Corresponding author. E-mail: lujun@mail.buct.edu.cn (J.L.); weimin@mail.buct.edu.cn (M.W.). Fax: +86-10-64425385. Phone: +86-10-64412131.

(1) Burroughes, J. H.; Bradley, D. D. C.; Brown, A. R.; Marks, R. N.; Mackay, K.; Friend, R. H.; Burns, P. L.; Holmes, A. B. *Nature* **1990**, *347*, 539.

(2) (a) Ho, P. K. H.; Granström, M.; Friend, R. H.; Greenham, N. C. *Adv. Mater.* **1998**, *10*, 769. (b) Ma, W.; Iyer, P. K.; Gong, X.; Liu, B.; Moses, D.; Bazan, G. C.; Heeger, A. J. *Adv. Mater.* **2005**, *17*, 274.

(3) Piris, J.; Kopidakis, N.; Olson, D. C.; Shaheen, S. E.; Ginley, D. S.; Rumbles, G. *Adv. Funct. Mater.* **2007**, *17*, 3849.

(4) (a) Amrutha, S. R.; Jayakannan, M. *J. Phys. Chem. B* **2008**, *112*, 1119. (b) Igor, A. L.; Jinsang, K.; Timothy, M. S. *J. Am. Chem. Soc.* **1999**, *121*, 1466.

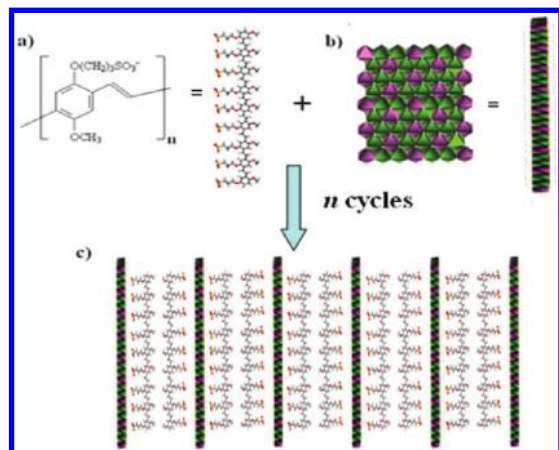
(5) (a) Chou, C. H.; Hsu, S. L.; Yeh, S. W.; Wang, H. S.; Wei, K. H. *Macromolecules* **2005**, *38*, 9117. (b) Xia, C.; Advincula, R. C. *Macromolecules* **2001**, *34*, 5854.

(6) Kim, S.; Jackiw, J.; Robinson, E.; Schanze, K. S.; Reynolds, J. R.; Baur, J.; Rubner, M. F.; Boils, D. *Macromolecules* **1998**, *31*, 964.

(7) (a) Fogg, A. M.; Green, V. M.; Harvey, H. G.; O'Hare, D. *Adv. Mater.* **1999**, *11*, 1466. (b) Choy, J. H.; Kwak, S.-Y.; Jeong, Y.-J.; Park, J.-S. *Angew. Chem., Int. Ed.* **2000**, *39*, 4041. (c) Yan, D. P.; Lu, J.; Wei, M.; Evans, D. G.; Duan, X. *J. Phys. Chem. B* **2009**, *113*, 1381.

(8) (a) Li, L.; Ma, R. Z.; Ebina, Y.; Iyi, N.; Sasaki, T. *Chem. Mater.* **2005**, *17*, 4386. (b) Liu, Z. P.; Ma, R. Z.; Osada, M.; Iyi, N.; Ebina, Y.; Takada, K.; Sasaki, T. *J. Am. Chem. Soc.* **2006**, *128*, 4872.

Scheme 1. (a) Chemical Formula of APPV, (b) Representation of One Monolayer of Mg–Al-Layered Double Hydroxide (Mg–Al-LDH)^a, and (c) Resulting (APPV/LDH)_n UTFs



^a Dark pink, Al(OH)₆ octahedra; green, Mg(OH)₆ octahedra.

ultrathin films (UTFs) with combining the properties of organic polymers with those of inorganic parts. Furthermore, it can be predicted that the π -CP/LDH UTFs will be a kind of novel luminescence materials with the following advantages: (1) The LDH monolayer provides π -CP with rigid and ordered micro-environment to isolate the polymer chains from each other between adjacent layers and thus eliminates the interlayer π - π stacking interaction. (2) The confined space imposed by LDH monolayers can suppress the thermal vibration of π -CP backbones relating to the nonradiative relaxation process of their exciting states. (3) The presence of inorganic LDH monolayers may improve the thermal and optical stability of the interlayer π -CPs.^{7c} (4) The assembly of π -CP and LDH monolayers can construct a periodic ordered layered structure, due to the intrinsic crystalline characteristic of the LDH monolayer. Moreover, the UTF systems may give rise to a new type of a multiple quantum well (MQW) structure, based on the energy-level match of the two building blocks (π -CP and LDH monolayer). The properties mentioned above have emerged as new potential characters for self-assembly functional UTF systems and could not be achieved by a typical polyanion/polycation UTF.

In our previous work, the anionic poly(*p*-phenylene) (APPP) and LDH monolayer were alternatively assembled into an (APPP/LDH)_n UTF by the LBL method.⁹ However, detailed photoemission and electrochemistry properties of the UTFs dependent on the assembled bilayer numbers and whether the LDH monolayers can impose the similar effort on other photoactive π -CPs remain unresolved. Herein, we further reported the ordered alternative assembly of a sulfonated derivative of PPV (poly(5-methoxy-2-(3-sulfopropoxy)-1,4-phenylenevinylene), APPV) and an exfoliated Mg–Al-LDH monolayer by the LBL method. The obtained (APPV/LDH)_n ($n = 4–32$) UTFs (Scheme 1) show long-range ordered structure and well-defined yellow fluorescence. Moreover, they exhibit longer fluorescence lifetime and higher photostability for UV irradiation than those of the drop-casting APPV film sample, and the polarized photoluminescence characteristics was nearly independent of the assembled number. A combination study of cyclic voltammetry (CV) with periodic density functional theoretical (DFT) calculation demonstrates that the APPV/LDH UTF is a kind of organic–inorganic hybrid MQW structure with low band energy,

where the valence electrons of APPV are confined and stabilized into the energy wells formed by the inert LDH monolayers. Therefore, this work provides a feasible route for the design of MQW architecture with potential luminescence application based on the organic π -CP and inorganic LDH components.

Experimental Section

Reagents and Materials. Analytical pure Mg(NO₃)₂·6H₂O, Al(NO₃)₃·9H₂O, and urea were purchased from Beijing Chemical Co. Ltd. and used without further purification. Poly[5-methoxy-2-(3-sulfopropoxy)-1,4-phenylenevinylene] potassium salt (APPV) was purchased from Sigma Chemical Co. Ltd.

Fabrication of (APPV/LDH)_n UTFs. The processes of synthesis and exfoliation of Mg–Al-LDH were similar to that described in our previous work.⁹ A total of 0.1 g of Mg–Al-LDH was shaken in 100 cm³ of formamide solution for 24 h to produce a colloidal suspension of exfoliated Mg–Al-LDH nanosheets. The quartz glass substrate was first cleaned in concentrated NH₃/30% H₂O₂ (7:3) and concentrated H₂SO₄ for 30 min each. After each procedure, the quartz substrate was rinsed and washed thoroughly with deionized water. The substrate was dipped in a colloidal suspension (1 g dm⁻³) of LDH nanosheets for 10 min followed by washing thoroughly, and then the substrate was treated with a 100 mL of APPV aqueous solution (0.025 wt %) for 10 min, and the washing procedure of APPV was the same as that for the LDH nanosheets described above. Multilayer films of (APPV/LDH)_n were fabricated by depositing alternatively with LDH nanosheets suspension and APPV solution for n cycles. The resulting films were dried under a nitrogen gas flow for 2 min at 25 °C. The comparison sample of drop-casting APPV films were prepared by the solvent evaporation method, which shows comparable photoluminescence intensity with the (APPV/LDH)₁₆ UTF.

Sample Characterization. The UV–vis absorption spectra were collected in the range from 190 to 800 nm on a Shimadzu U-3000 spectrophotometer, the width of the slit is 1.0 nm. The fluorescence spectra were performed on RF-5301PC fluorospectrophotometer with the excitation wavelength of 429 nm. The fluorescence emission spectra range in 450–700 nm, and both the excitation and emission slits are set to 3 nm. The in situ fluorescence measurement for UV-light-resistance capability of the films was performed with slits of 10 nm for both excitation and emission. Steady-state polarized photoluminescence measurements of APPV/LDH were recorded with an Edinburgh Instruments' FLS 920 fluorospectrophotometer. The fluorescence decays were measured using a LifeSpec-ps spectrometer with a 372 nm excitation laser for the APPV/LDH films, and the lifetimes were calculated with the F900 Edinburgh Instruments software. X-ray diffraction patterns (XRD) of APPV/LDH UTFs were recorded using a Rigaku 2500 VB2+PC diffractometer under the conditions: 40 kV, 50 mA, Cu K α radiation ($\lambda = 0.154056$ nm) step-scanned in steps of 0.04° (2θ) in the range from 2 to 12° using a count time of 10 s/step. The morphology of thin films was investigated by using a scanning electron microscope (SEM Hitachi S-3500) equipped with an EDX attachment (EDX Oxford Instrument Isis 300), and the accelerating voltage applied was 20 kV. The surface roughness and thickness data were obtained by using the atomic force microscopy (AFM) software (Digital Instruments, version 6.12). Electrochemical measurements were performed with the model 1100A electrochemical analyzer (CH Instruments) using indium tin oxide (ITO) glass as the working electrode, platinum wire as the auxiliary electrode, and Ag/Ag⁺ as the reference electrode. Cyclic voltammetry (CV) studies of the (APPV/LDH)_n ($n = 4–32$) deposited on ITO were carried out at a scan rate of 100 mV s⁻¹ and in *N,N*-dimethylformamide solution containing 0.1 M of Bu₄NBF₄ as supporting electrolyte. With the use of the onset electric potentials in the CV curves, the LUMO (lowest unoccupied molecular orbital) and HOMO (highest occupied molecular orbital) energy levels can be determined.

(9) Yan, D. P.; Lu, J.; Wei, M.; Han, J. B.; Ma, J.; Li, F.; Evans, D. G.; Duan, X. *Angew. Chem., Int. Ed.* **2009**, *48*, 3073.

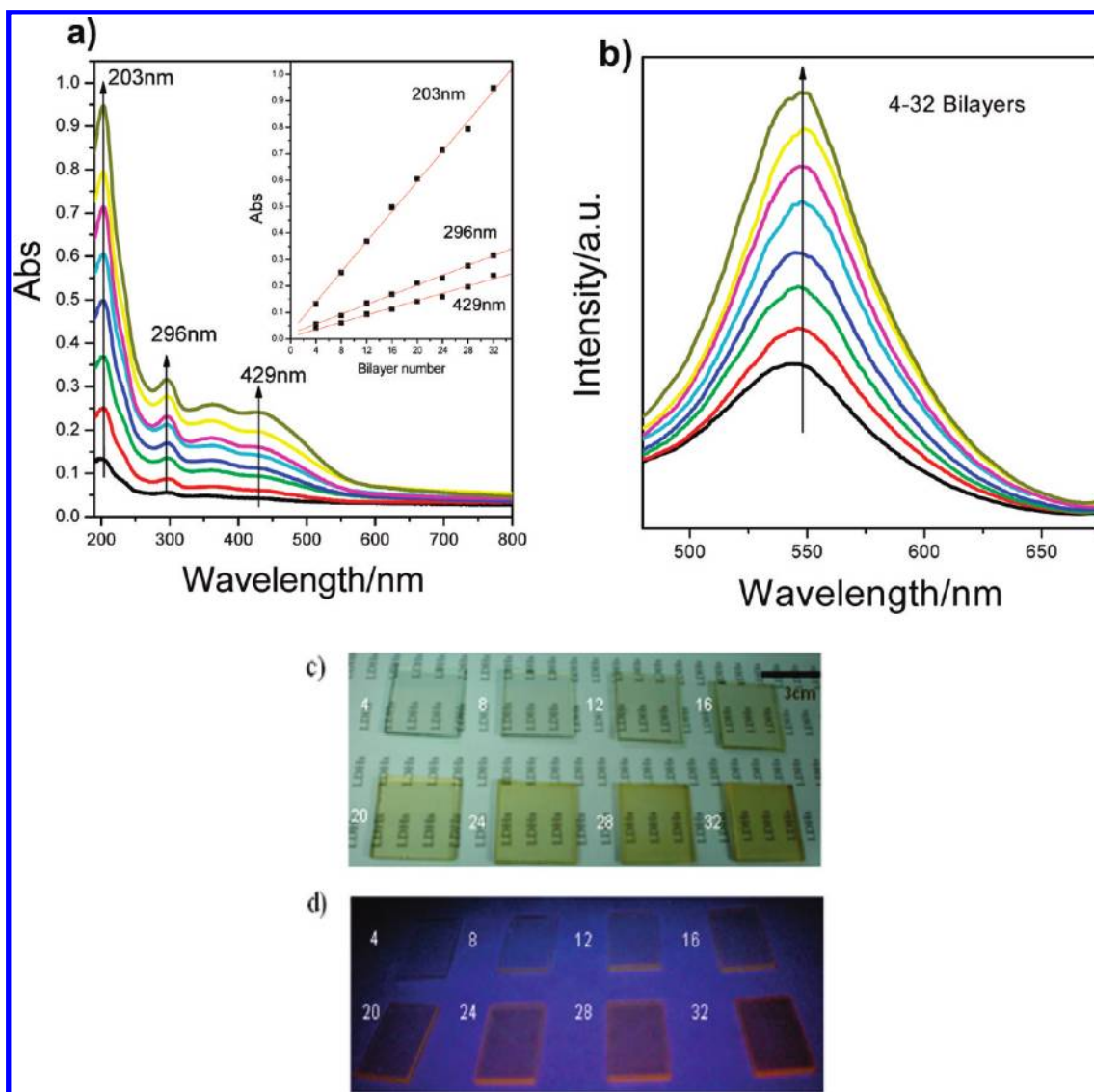


Figure 1. Characterization of $(\text{APPV/LDH})_n$ ($n = 4\text{--}32$) UTFs: (a) UV-vis absorption spectra (the inset shows the absorbance at 203, 296, and 429 nm vs n), (b) fluorescence spectra, and (c and d) photographs of UTFs with different bilayer numbers under daylight and UV light (365 nm), respectively.

Building of the Structural Model of APPV/LDH System and Computational Method. An ideal LDH layer with $R3m$ space group containing 12 Mg atoms and 6 Al atoms was built. The lattice parameters of the two-dimensional layer are $a = b = 3.05 \text{ \AA}$, which is in accordance with other literatures.¹⁰ Every octahedral layer has 18 metal atoms and 36 OH groups, and a supercell was constructed with lattice parameter $a = 18.30 \text{ \AA}$, $b = 9.15 \text{ \AA}$, and the initial interlayer spacing $c = 34 \text{ \AA}$, $\alpha = \beta = 90^\circ$, $\gamma = 120^\circ$ (equivalent to a $6 \times 3 \times 1$ supercell). The supercell was treated as $P1$ symmetry, and the three-dimensional periodic boundary condition was applied. Then, the representative of APPV, two anionic trimers ($\text{C}_{34}\text{H}_{39}\text{O}_{15}\text{S}_3$) with three negative charges each were introduced into the simulated supercell, in

which their sulfonatopropoxy groups are normal to the layers of LDH. As a result, the formula of the simulated structure can be expressed as $\text{Mg}_{12}\text{Al}_6(\text{OH})_{36}(\text{C}_{68}\text{H}_{78}\text{O}_{30}\text{S}_6)$. All calculations were performed with the periodic density functional theory (DFT) method using the Dmol3^{11a,b} module in the Material Studio software package.^{11c} The initial configuration was first fully optimized with fixed positions for the atoms in the layer by the classical molecular mechanics method employed a cff91 force field,^{11d-f} and then further optimization was implemented by the Perdew-Wang (PW91)^{11g} generalized gradient approximation (GGA) method with the double numerical basis sets plus polarization function (DNP). The core electrons for metals were treated by effective core potentials (ECP). SCF converged criterion was within 1.0×10^{-5} hartree/atom and converged criterion of structure optimization was 1.0×10^{-3} hartree/bohr. The Brillouin zone is sampled by $1 \times 3 \times 1$ k -points, and test calculations reveal that the increase of k -points does not affect the results.

Results and Discussion

1. Assembly of the APPV/LDH UTFs. Figure 1a shows the UV-vis absorption spectra of $(\text{APPV/LDH})_n$ UTFs with various bilayer numbers (n) deposited on quartz substrates. It was

(10) (a) Mohanambe, L.; Vasudevan, S. *J. Phys. Chem. B* **2005**, *109*, 15651. (b) Newman, S. P.; Williams, S. J.; Coveney, P. V.; Jones, W. J. *Phys. Chem. B* **1998**, *102*, 6710.

(11) (a) Delley, B. *J. Chem. Phys.* **1990**, *92*, 508. (b) Delley, B. *J. Chem. Phys.* **2000**, *113*, 7756. (c) *Dmol3 Module, MS Modeling*, version 2.2; Accelrys Inc.: San Diego, CA, **2003**. (d) Maple, J. R.; Hwang, M.-J.; Stockfisch, T. P.; Dinur, U.; Waldman, M.; Ewig, C. S.; Hagler, A. T. *J. Comput. Chem.* **1994**, *15*, 162. (e) Yan, D. P.; Lu, J.; Wei, M.; Li, H.; Ma, J.; Li, F.; Evans, D. G.; Duan, X. *J. Phys. Chem. A* **2008**, *112*, 7671. (f) Yan, D. P.; Lu, J.; Wei, M.; Ma, J.; Evans, D. G.; Duan, X. *Phys. Chem. Chem. Phys.* **2009**, *11*, 9200. (g) Perdew, J. P.; Chevary, J. A.; Vosko, S. H.; Jackson, K. A.; Pederson, M. R.; Singh, D. J.; Fiolhais, C. *Phys. Rev. B* **1992**, *46*, 6671.

observed that the absorption bands at about 203, 296 (absorption of phenylene ring), and 429 nm (π - π^* transition of APPV) linearly correlate with n (Figure 1a, inset), indicating a stepwise and regular film growth procedure, which was further confirmed by the gradual color enhancement upon the increase of bilayers (Figure 1c). The sharp fluorescence peak of one phonon (S_1 - S_0) transition¹² at 2.25 eV (547 nm) of (APPV/LDH) $_n$ UTF also displays a consistent increase with n , as shown in Figure 1b. There is no obvious red or blue shift of the fluorescence spectra for the as-prepared UTF with different bilayers compared with the APPV pristine solution (Figure S1 in the Supporting Information), which indicates no formation of APPV aggregates throughout the whole assembly process. This can also be visualized by irradiating the thin films with UV light (Figure 1d), where these films exhibit uniform enhanced yellow luminescence with increasing n . The fluorescence lifetimes of (APPV/LDH) $_n$ UTFs range from 0.66 to 0.81 ns (Table S1 in the Supporting Information), comparable with that of the pristine APPV solution (0.60 ns). All these suggest that the rigid LDH monolayers isolate the polymer chains from each other and thus eliminate the interlayer π - π stacking interaction.

2. Morphology and Structural Characterization. The deposited process of (APPV/LDH) $_n$ UTFs was further monitored by atomic force microscopy and scanning electron microscopy (AFM and SEM, Figure S2 in the Supporting Information). The roughness and thickness of the as-prepared UTFs ($n = 8$ –32) are in the range of 6.5–12.2 and 36–120 nm, respectively (see Table S2 in the Supporting Information). The approximately linear increase of the thickness upon increasing the bilayer number confirms that the UTFs present uniform and periodic layered structure, in agreement with the behaviors revealed by the absorption and fluorescence spectra above. A typical top view of the SEM image for (APPV/LDH) $_{32}$ UTF (Figure 2a,b) shows that the film surface is microscopically smooth and uniform; moreover, the continuous and homogeneous UTF can also be observed from its side view of the SEM image (Figure 2c), with the thickness of 120 nm (Figure 2d). It thus can be estimated that the thickness of one bilayer (APPV/LDH) $_1$ is ~ 3.8 nm. The AFM topographical images as shown in parts e ($10 \mu\text{m} \times 10 \mu\text{m}$) and f ($2 \mu\text{m} \times 2 \mu\text{m}$) of Figure 2 give the morphology and roughness information of the UTF, from which it can be concluded that the film surface is relatively smooth with a root-mean square roughness of 12.19 nm. Additionally, plenty of “spherical” islands with nearly the same size (~ 330 nm) are clearly resolved on the UTF surface, which may be attributed to the ordered stacks of APPV/LDH microcrystallites. Furthermore, the UTF shows a homogeneous brightness of yellow under the fluorescence microscope (Figure 2g,h), indicating the uniform distribution of APPV chromophores throughout the film. X-ray diffraction peaks of the as-prepared UTFs appear at ~ 2.5 – 2.7° , and the peak intensity increase upon the increasing bilayer number indicate that the UTF is an orderly periodical structure in the normal direction of the film with a period of 3.3–3.5 nm (Figure 3a and Table S3 in the Supporting Information), and this value is approximately consistent with the thickness augment per deposited cycle observed by SEM. Moreover, this is also in agreement with the ideal double-layered arrangement model of the APPV/LDH supramolecular structure with the thickness of about 0.48 nm for a monolayer of LDH and 1.28 nm for the extended chain configuration of APPV (Figure 3b). The little decrease of the d value for the (APPV/LDH) $_{32}$ UTF compared

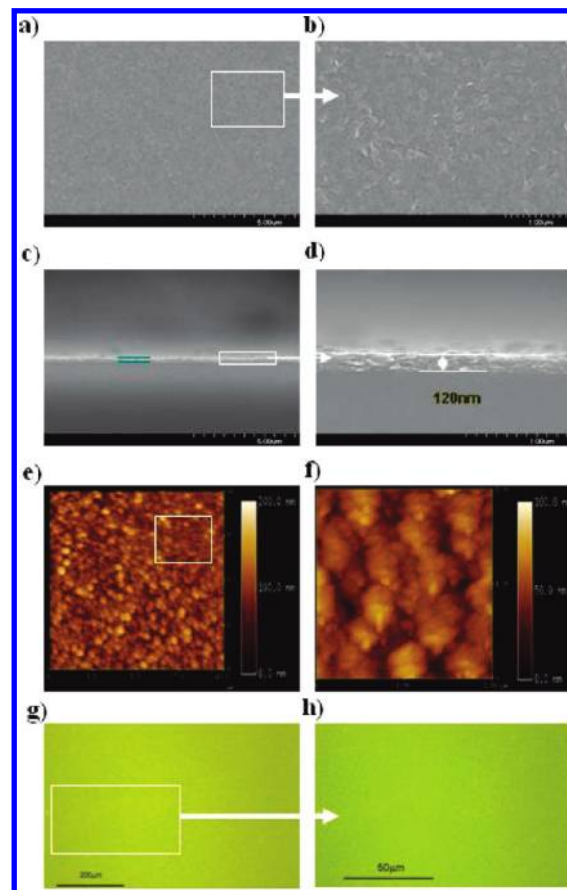


Figure 2. The morphology of (APPV/LDH) $_{32}$ UTF for (a, b) top view of the SEM image, (c, d) side view of the SEM image, (e, f) tapping-mode AFM topographical image, and (g, h) fluorescence microscope image.

with others can be attributed to the fact that the compact degree of the APPV in the LDH gallery has increased upon the increasing bilayers number.

3. Polarized Fluorescence of the UTFs. To further investigate the microenvironment of the APPV polymers in the as-prepared UTFs with variable bilayers, a polarized fluorescence measurement was employed to probe the fluorescence anisotropic value r .¹³ Two typical measurement setups of polarized fluorescence (glancing and normal incidence geometry as shown in Figure S3 in the Supporting Information) were employed to determine the fluorescence anisotropic value r . It was observed that, for the in-plane polarized excitation light, the (APPV/LDH) $_8$ UTF shows well-defined yellow fluorescence anisotropy between the parallel and perpendicular to excitation polarized direction (I_{VV} vs I_{VH}) with the anisotropic value (r) of 0.25–0.30 (slightly less than the highest value of 0.4 for the system without macroscopic alignment¹⁴). The I_{VV}/I_{VH} ratio is 1.88 (Figure S3a in the Supporting Information), larger than that of the vertical excitation and horizontal emission mode by $\sim 45\%$ (Figure S3b in the Supporting Information). The uniform r value ranging in 500–600 nm indicates that polarization scrambling via Förster

(13) (a) Yan, D. P.; Lu, J.; Wei, M.; Ma, J.; Evans, D. G.; Duan, X. *Chem. Commun.* **2009**, 6358. (b) $r = (I_{VV} - GI_{VH}) / (I_{VV} + 2GI_{VH})$, where $G = I_{HV}/I_{HH}$, determined from the APPV aqueous solution. I_{VH} stands for the photoluminescence intensity obtained with vertical excitation polarized and horizontal detection polarization, and I_{VH} , I_{HV} , and I_{HH} are defined in a similar way.

(14) Clark, A. P.-Z.; Shen, K.-F.; Rubbin, Y. F.; Tolbert, S. H. *Nano Lett.* **2005**, *5*, 1647.

(12) Kim, S. T.; Hwang, D.; Li, X. C.; Grüner, J.; Friend, R. H.; Holmes, A. B.; Shim, H. K. *Adv. Mater.* **1996**, *8*, 979.

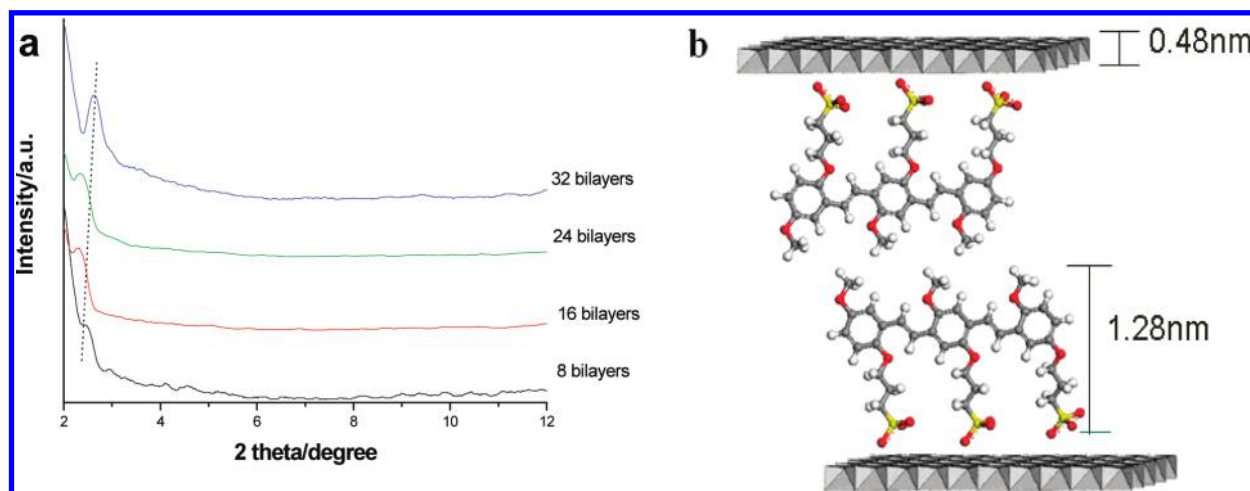


Figure 3. (a) Small angle XRD patterns for the $(\text{APPV/LDH})_n$ UTFs with 8, 16, 24, and 32 bilayers and (b) structural model of APPV/LDH.

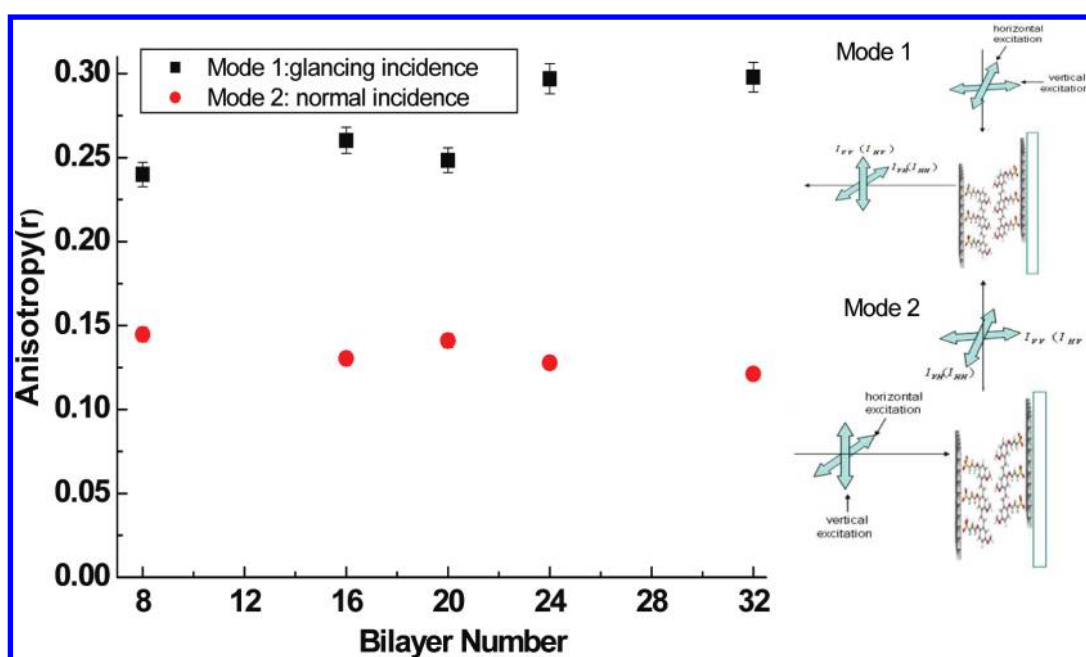


Figure 4. The correlation between fluorescence anisotropic values (r) of APPV/LDH UTFs (averaged in the range 500–600 nm) and the bilayer number in two measurement modes (glancing and normal incidence geometry).

transfer is minimal in the UTF and also confirms the rigid-rod and isolated conformation of the APPV chains within the gallery. Furthermore, the r value is nearly independent of the bilayer number in the two measurement modes (Figure 4). This indicates that the film thickness imposes no obvious influence on the macroscopic polarized luminescence characteristics of APPV/LDH UTFs with different bilayers throughout the whole assembly process.

4. Photostability of the UTF. It is more illuminating to further compare the photophysical properties of APPV/LDH UTFs with the pristine APPV film prepared by the traditional drop-casting method. Compared with the APPV pristine solution, the fluorescence peak of the drop-casted APPV film shows a redshift by ~ 5 – 7 nm, which may be induced by π – π interaction of the APPV polymer backbones. Moreover, the fluorescence lifetime of the drop-casted film (0.21 ns) was lower than the APPV/LDH UTFs by a factor of 3–3.85, further demonstrating that the nonradiative relaxation of APPV in the excited state could be effectively suppressed when located between the rigid LDH

monolayers. To further investigate the optical stability of the two APPV-based films, an in situ photoluminescence measurement was performed for the $(\text{APPV/LDH})_{16}$ UTF and drop-casted APPV film with very close fluorescence intensity. After continuous irradiation with UV light (360 nm) for 2 min, the fluorescence intensity falls down by $\sim 3\%$ and 15% for the $(\text{APPV/LDH})_{16}$ UTF and drop-casted APPV film, respectively (Figure S4 in the Supporting Information). Moreover, the normalized fluorescence intensities of $(\text{APPV/LDH})_{16}$ are systematically larger than the counterpart (Figure 5), implying that the APPV/LDH UTF exhibits a better UV-light-resistance capability than the pristine drop-casted APPV film.

5. Electrochemistry Characteristics of the UTFs. Cyclic voltammetry measurements of the $(\text{APPV/LDH})_n$ UTFs ($n = 4$ – 32) were performed to analyze their electronic structure, and it was found that both the oxidation and reduction electric potentials ($E_{\text{onset,ox}}$ and $E_{\text{onset,red}}$) of APPV/LDH UTFs increase systematically upon increasing the bilayer number (Figures S5 and S6 in the Supporting Information). Accordingly, on the basis

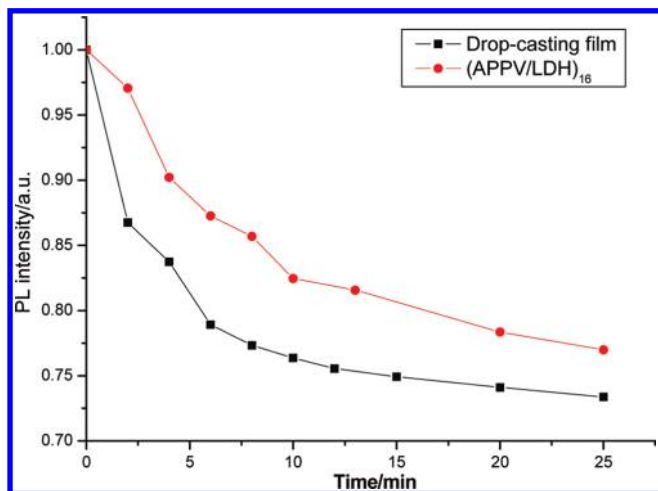


Figure 5. The decay of the normalized maximal PL intensity along with time for probing the UV-light-resistance capability of the drop-casted film and (APPV/LDH)₁₆ UTF, both of which were irradiated with UV light of 360 nm under the same conditions.

of the empirical relationships proposed by Leeuw et al.,¹⁵ the frontier orbitals (the highest occupied molecular orbital (HOMO) and lowest unoccupied molecular orbital (LUMO)) energy can be determined as follows:

$$E(\text{HOMO}) = -(E_{\text{onset, ox}} + 4.39)(\text{eV})$$

$$E(\text{LUMO}) = -(E_{\text{onset, red}} + 4.39)(\text{eV})$$

Therefore, the band gap energy can be calculated by $\Delta E_{\text{g}} = E(\text{LUMO}) - E(\text{HOMO})$, and it was found that the HOMO and LUMO energies of the APPV/LDH system decreases by ~ 7 meV with the increase of one assembled cycle, and the HOMO energy of APPV/LDH UTFs (from -5.69 to -5.85 eV) are totally lower than that of the pristine APPV film (-5.65 eV) as shown in Figure 6. This trend suggests that the valence electrons of APPV can be stabilized by the LDH monolayer, and the hole transporting ability of APPV was improved effectively.^{5b} This effect becomes more remarkable for the APPV/LDH UTF upon increasing the bilayer number. Meanwhile, the band gap energy (ΔE_{g}) of the UTFs nearly keeps constant (Table S4 in the Supporting Information) with the average value of 1.83 eV.

6. Calculated Electronic Structure. To further study the electronic structure of the APPV/LDH system, a periodic density functional theoretical (DFT) calculation was employed for the ideal model of the APPV/LDH structure. The optimized geometry of the APPV/LDH system was shown in parts a and b of Figure 7 for the side and top view images, respectively. The APPV main chains run along the $[1 -2 0]$ direction of the supercell, in agreement with the aligned direction of positive charges located in the ideal LDH monolayer. The energy band calculation shows (see Figure S7 in the Supporting Information) that the APPV/LDH system exhibits a low band gap of 1.74 eV at the Γ point (0,0,0) in the first Brillouin Zone (BZ), close to that of the experimental observation for both the pristine APPV and the APPV/LDH film. The energy bands around the Fermi levels show almost complete independence on the k electron wave vectors

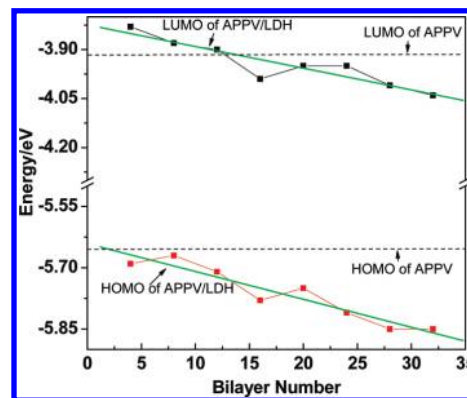


Figure 6. Frontier orbital (HOMO and LUMO) energy of the APPV/LDH UTF as a function of bilayer number obtained from the CV measurement. The corresponding energies of the pristine APPV film were marked as the dashed lines.

along the ΓZ line ($[001]$ direction), indicating the strong valence electron confinement effect on the host layer in the normal direction. The highest valence electron dispersion mainly occurs along the ΓN line (the main chain of APPV), suggesting the existence of electron delocalization in the main chain of APPV. In addition, the weak dependence of k on band energy along the ZM line (the direction perpendicular to the main chain of APPV) indicates that the APPV polymers exhibit no obvious interaction and thus disperse homogeneously in the gallery formed by LDH monolayers.

Total electronic densities of states (TDOS) and partial electronic densities of states (PDOS) analysis (Figure 7c and Figure S8 in the Supporting Information) reveal that the top of valence band (TVB) and the bottom of conducting band (BCB) are mainly dominated by the $2p(\pi)$ and $2p(\pi^*)$ carbon atomic orbitals from APPV molecules, respectively. Around the Fermi level, the TDOS mainly consisted of the $2p$ electrons of C atoms in APPV. The O $2p$ and Mg/Al $3s$, H $1s$ orbitals from the LDH monolayers contribute to the TDOS below and above the TVB and BCB, respectively, with the gap of 5.7 eV. Therefore, the photo excitation process mainly occurs in the main chain of the APPV molecule, whereas the Mg–Al–LDH monolayers remain inert. This further indicates that the valence electrons localized in the APPV main chains are confined due to the energy blocking action of the LDH monolayers. Therefore, the APPV/LDH UTF serves as a multiple quantum well (MQW) structure, which is beneficial to the stabilization of the valence electronic orbital energy for photoactive polymers, as described in the CV experiment. Moreover, although MQW structures have been greatly investigated in pristine inorganic^{16a} and organic^{16b} systems, there are very few observations of such structure based on both organic and inorganic components.^{16c} This work demonstrates that the as-fabricated APPV/LDH UTF can be regarded as organic–inorganic hybrid MQW. Compared with the traditional inorganic MQW, the interactions of two alternate layers in the organic–inorganic MQW are mainly electrostatic and/or van der Waals force, without the prerequisites of lattice matching. Furthermore, the organic–inorganic MQW could exhibit more structural order and better photostability than the organic MQW fabricated by a polyanion/polycation film.

(15) (a) deLeeuw, D. M.; Simenon, M. M. J.; Brown, A. R.; Einerhand, R. E. F. *Synth. Met.* **1997**, *87*, 53. (b) Chen, Z. K.; Huang, W.; Wang, L. H.; Kang, E. T.; Chen, B. J.; Lee, C. S.; Lee, S. T. *Macromolecules* **2000**, *33*, 9015.

(16) (a) Kim, H.-M.; Cho, Y.-H.; Lee, H.; Kim, S.; Ryu, S. R.; Kim, D. Y.; Kang, T. W.; Chung, K. S. *Nano Lett.* **2004**, *4*, 1060. (b) Hong, H.; Tarabia, M.; Chayet, H.; Davidov, D.; Faraggi, E. Z.; Avny, Y.; Neumann, R.; Kirstein, S. *J. Appl. Phys.* **1996**, *79*, 3082. (c) Tim. R. *Nat. China*, **2009**, DOI: 10.1038/nchina.2009.76.

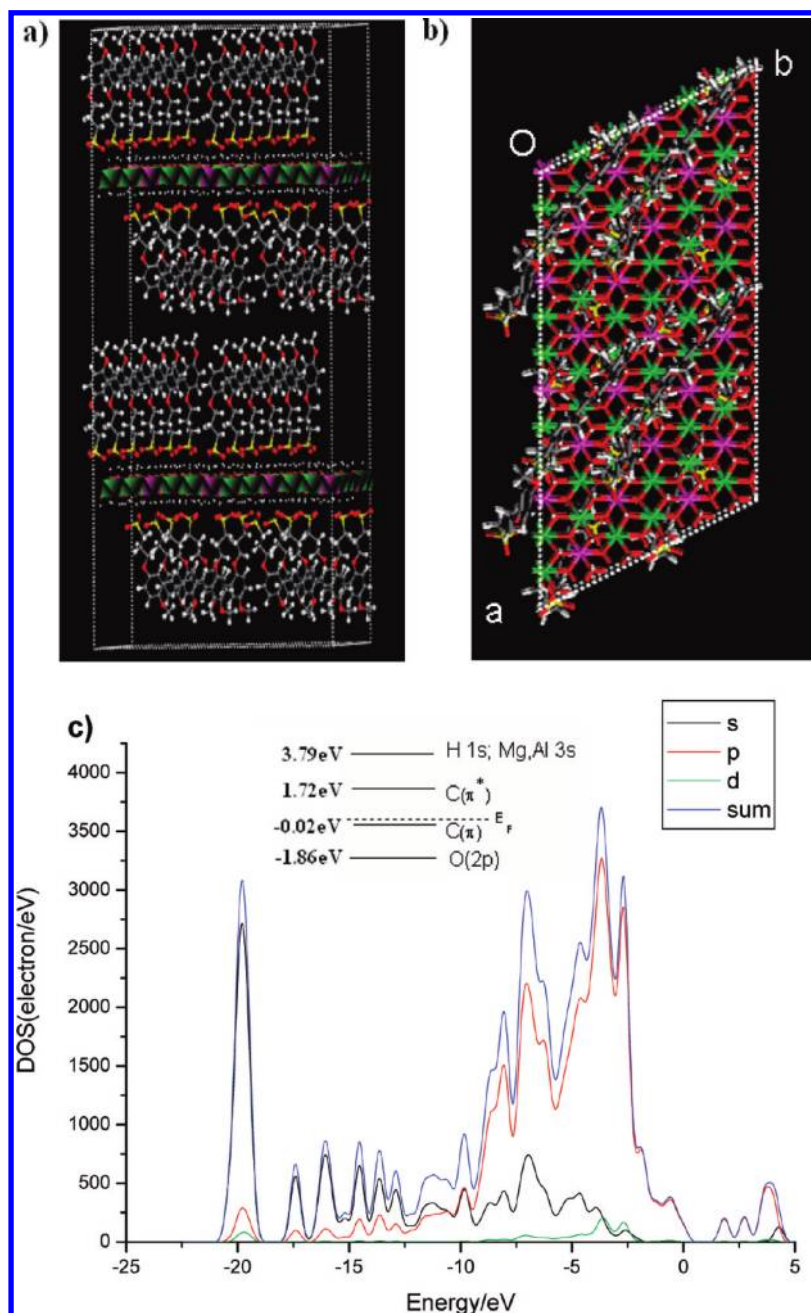


Figure 7. (a) side and (b) top view of the DFT optimized structure of the APPV/LDH system (white, H; pink, Al; red, O; purple, Mg; gray, C; yellow, S). The $6 \times 3 \times 1$ supercell for calculation was outlined; (c) total and partial electronic density of state (TDOS and PDOS) for the APPV/LDH system. The Fermi energy level (E_F) was set as zero.

Conclusions

In summary, the ordered (APPV/LDH) $_n$ UTFs were fabricated in this work, which show well-defined yellow photoluminescence and comparable fluorescence lifetime with the APPV solution. Moreover, the existence of LDH monolayer leads to higher UV photostability and lower valence electron energy for the APPV, confirming that the LDH monolayers improve the luminescence properties of APPV by suppressing the π - π stacking of polymer backbones. The DFT calculation demonstrates that the APPV/LDH UTF has a low band gap. No electron delocalization occurs between the APPV and LDH monolayer at the top of the valence band, indicating that the LDH monolayer functions well as an energy blocking layer, which hampers the interlayer interaction of the APPV chains as experimental observation. As a result, the

UTF can be regarded as a new type of organic–inorganic hybrid MQW structure. It can be expected that by tuning and controlling the component, diversity and alignment of π -CPs in the energy wells formed by the LDH monolayers with different electrostatic assembly architecture, double-color and multicolor light-emitting UTFs with improved light-emitting efficiency can be constructed. Moreover, the LDH energy barrier of the MQW can be tuned in heights and/or widths by assembling LDHs monolayers with different charge density. This work opens new ways to design, construct, and investigate novel organic–inorganic MQW structures for the fabrication of π -CP-based opto-electrical devices.

Acknowledgment. This work was supported by the National Natural Science Foundation of China, the 111 Project (Grant No.: B07004), the 973 Program (Grant No. 2009CB939802)

and the “Chinese Universities Scientific Fund” (Grant No.: ZZ0908).

Supporting Information Available: Emission spectrum of APPV aqueous solution; fluorescence lifetimes of the (APPV/LDH)_n UTFs with monoexponential fitting; depth and thickness parameters for the UTFs; side view of the SEM image for APPV/LDH UTFs; 2θ degree and *d* values (in Angstroms) for (APPV/LDH)_n UTFs; polarized fluorescence spectra for the (APPV/LDH)₈ UTF; in situ PL

spectra under UV-irradiation of APPV/LDH UTF and the drop-casted APPV film; cyclic voltammetry of (APPV/LDH)_n UTFs and the drop-casted APPV film; experimental values of the band gap energy for the (APPV/LDH)_n UTFs; oxidation and reduction electric potential of (APPV/LDH)_n UTFs; calculated band structure around the Fermi energy level of the APPV/LDH system; and partial electronic densities of states (PDOS) of different atoms in the APPV/LDH system. This material is available free of charge via the Internet at <http://pubs.acs.org>.